Comparison of Simulation Snapshots To CO Emission of M83 and Exploring The Tremaine Weinberg Method to Determine The Pattern Speed of the Galaxy

J. Koda[1], S. A. H. Shanto[1], and J. Caputi[1]

[1]*Department of Physics & Astronomy, SUNY Stony Brook, Stony Brook, NY 11794-3800, USA*

Summer Research 2021

Abstract

Simulation data can give us significant information beyond the limits of observational data. However the simulation data itself needs to be calibrated to match the observation data to provide the most accurate data. The main prospect of our research was to compare density and iso-contour simulation time snapshots to CO emission snapshots of galaxy M83. The best match provided us with necessary parameters required to determine the pattern speed of M83 by using the Tremaine Weinberg method. We used both gas and star particle data to determine the pattern speeds of the galaxy.

1   Introduction

The structure and nature of the arms in spiral galaxies are still an open question. The Density wave theory has been an exciting proponent in explaining the spiral arms of galaxies since the mid-1960s. Lin and Shu [1964] first proposed the approach. Their idea was that a galaxy's spiral structure was not material; instead, they were long-lived quasi-stationary density waves that create a semi-permanent spiral structure on the face of a galactic disk. The theory also implies that star formation can be triggered due to gas compression as the gas passes through the density enhancement in the spiral arm. However, such a long-lived quasi-stationary structure would only exist if the pattern moved with a constant angular speed, more commonly known as pattern speed, Ω_p. Therefore, pattern speed is a fundamental parameter for testing The Density Wave theory and is also one of the main motivations behind our research. However, it is has been proven somewhat elusive to determine pattern speed from direct observation.

A more indirect but rather conclusive approach to determining pattern speed was developed by Tremaine and Weinberg [1984]; (hereafter TW). A version of

the method that we found suitable for our research was refined by Merrifield and Kuijken [1995]. Their approach requires parameters such as inclination angle of the galaxy, intensity weighted average line of sight velocity, and intensity weighted average of the major axis to determine the pattern speed of the galaxy. The theoretical segment of our research focused on these parameters from simulation data of the galaxy M83.

The primary part of our research was determining a density and velocity snapshot from simulation data that matched the CO emission snapshots of the galaxy. Such a procedure would not only lead to a fair comparison of pattern speed between observation and simulation data but also help to verify the simulation as a whole. After the determination of the best match, data cubes can be generated from the plots. Then the required parameters(intensity weighted average line of sight velocity and intensity weighted average of the major axis) obtained from the 3D cubes can be used to determine the pattern speed of the galaxy. We discuss the whole research procedures and TW method in more detail in the method segment, then discuss and conclude our findings in the discussion segment.

2   The Tremaine Weinberg Method

The Tremaine Weinberg method, is a straightforward method that uses readily observable quantities to determine the density wave pattern speed, Ω_P, along the minor axis of barred and spiral galaxies. The method was first introduced by Tremaine and Weinberg [1984] and is based on five major conditions:

- The disc of the galaxy is flat; at least up to the region of the galaxy where the intensity of the tracer is nearly zero.

- The whole galaxy has one well defined pattern speed.

- There is a well defined surface mass density tracer for the galaxy from which the intensity of the tracer can be obtained. The radial velocity is also known.

- The surface density of the of the galaxy must go to zero at the edges of the galaxy.

- The surface brightness of the tracer follows the continuity equation over several orbits of the galaxy.

The equation for the last condition can be written as:

$$\frac{\delta\Sigma(x,y,t)}{\delta t} + \frac{\delta}{\delta x}[\Sigma(x,y,t)v_x(x,y,t)] + \frac{\delta}{\delta y}[\Sigma(x,y,t)v_y(x,y,t)] = 0$$

Here Σ is the surface density; v_x and v_y are velocity components in Cartesian coordinates. So if we rewrite the equation with polar coordinates, constant

2

pattern speed Ω_P and placing the velocity components in the right hand side of the equation, we should get :

$$\frac{\delta\Sigma}{\delta t} = \frac{\delta\Sigma}{\delta\phi}\frac{\delta\phi}{\delta t} = -\Omega_P\frac{\delta\Sigma}{\delta\phi} - \Omega_P(x\frac{\delta\Sigma}{\delta y} - y\frac{\delta\Sigma}{\delta x})$$

Now if we make Ω_P, the subject and combine equation find and second equation; by replacing the time dependant surface density, we get:

$$\Omega_P = \frac{\delta(\Sigma v_x)/\delta x + \delta(\Sigma v_y/\delta y)}{x(\delta\Sigma/\delta y) - y(\delta\Sigma/\delta x)}$$

The TW method shows that the terms involving the derivatives of x gets cancelled when we integrate the numerator and denominator from $x = -\infty$ to $+\infty$, this yields:

$$\Omega_p = \frac{\int_{-\infty}^{+\infty}[\Sigma v_y/\delta y]dx}{\int_{-\infty}^{+\infty} x(\delta\Sigma/\delta y)dx}$$

Even though this equation is intuitive the parameters still depend on the y derivative, which is calculable but noisy so we integrate again to eliminate dy and have an equation that use readily usable parameters:

$$\Omega_p = \frac{\int_{-\infty}^{+\infty} \Sigma v_y dx}{\int_{-\infty}^{+\infty} x\Sigma dx}$$

Now with accordance to the third condition, we have $I(x) \propto \Sigma(x)$ and $v_y \sin i = v_{LOS}$, where v_{LOS} is the line of sight velocity, so plugging these in the equation gives us:

$$\Omega_p = \frac{1}{\sin i}\frac{\int_{-\infty}^{+\infty} I(x)v_{LOS}dx}{\int_{-\infty}^{+\infty} xI(x)dx}$$

Merrifield and Kuijken(1995) normalised the numerator and denominator using the total intensity. The refined version of the TW method yields:

$$\Omega_p = \frac{1}{\sin i}\frac{<V(x)>}{<x>}$$

Here $<V(x)>$ is intensity weighted average line of sight of velocity, $<x>$ is the the intensity weighted average of the major axis and i is the inclination angle of the galaxy. Finally, this version makes it feasible enough for simulation and observation data cubes to provide the readily available parameters. Which then can be used to determine the pattern speed,Ω_P, of the galaxy. The refinement avoids the problem leading to singularity where the denominator may go to zero near the center of the galaxy. The adverse effects of the orginal TW method such as errors in the dynamical center and systemic velocity approximations are also omitted due to this refinement. A more detailed approach to how we used these 3D data cubes and parameters to determine the pattern speed of M83 is described below.

3 Method

3.1 Generating Snapshots from Simulation Data

The first and most significant part of the research was determining a time snapshot of the galaxy M83 from simulation data. Such a procedure would verify the simulation and provide a substantial source of simulation data to determine pattern speed. We produced two snapshots, density, and iso-contour velocity, to compare with the snapshots from CO emission of the galaxy.

We used python scripts to generate both plots. To make the density plot, we selected the number of grid cells to be 256 along both the x and y-direction. We also chose the range of the x-axis and y-axis to be 35 kpcs; choosing a smaller value keeps the focus on the galaxy's central(arms and bar) region. We mainly used gas-particle data for the plots; however, we also used stellar particle data later in the research, e.g., for pattern speed determination. A rotation matrix was applied to transform the data along the inclination angle of 26 degrees, node angle of 0 degrees, and position angle of 45 degrees. The node angle was to be varied later for comparison purposes. The boundaries for the plot were then calculated by dividing the grid cell number in half. The grid spacing was calculated by subtracting the upper boundary with the lower boundary and dividing the result by the number of grid cells. The cell number in each direction was then calculated by subtracting the upper boundary from the simulation parameter value and then dividing the result by the grid spacing. Finally, the cell position of all particles was calculated by multiplying the cell number in the y-direction with the grid cells along the x-axis and then adding the result with the cell number along the x-direction. A histogram function was then used to integrate cell position in each direction and output a one-dimensional array. This trick speeds up the process, especially in comparison to manually adding up each cell. We used the mass of the particles as weights for the histogram. The array from the histogram was then reshaped into a two-dimensional image. Finally, we used the image show function from the Matplotlib library to generate a density plot of the galaxy.

The iso-contour velocity plots, however, required a bit more complexity. Along with the x and y grid cells, a line of sight velocity, vz grid cells with a value of 64, were added along the z-direction. Grid cell values along the x and y-axis were again selected to be 256. We chose the value of the vz axis to be 600 km/s which covers most of the velocities. The range of the x and y-axis remained the same as density plots. Boundaries were calculated in a similar manner by dividing the grid cell numbers in half. Simulation parameters were imported, and then a rotation matrix was applied to transform the data along the inclination angle of 26 degrees, node angle of 0 degrees, and position angle of 45 degrees. Grid spacing for the parameters was calculated in a similar fashion to the density plots, but in this case, the vz parameter was also included. The cell position was calculated by multiplying the vz cell number with y grid cells and adding y cell number, then multiplying the result with x grid cells and adding the x cell number. The histogram function was an essential trick for the velocity

plot, producing the mass-weighted velocity array. For this purpose, we used two histogram functions. The first histogram function integrated the cell position with weights as mass multiplied by the vz parameter from the simulation data. The second histogram function integrated the cell position with weights as mass only. Then the first histogram was divided by the second histogram, producing the one-dimensional mass-weighted velocity array. The array was then reshaped into a three-dimensional image. Then we used the image data to generate a filled contour imposed over a general contour. Enforcing the plot on one another made the velocity dispersion more apparent. For further enhancement, we positioned the iso-contour plot on top of the density plot. This procedure made the velocity dispersion of components in the galaxy more distinguishable.

After generating the density and velocity plots, they were positioned side by side using the subplot function from the Matplotlib library. In the end, there were around 300 time snapshots, and we had to check the node angle for each time snapshot from 0 to 360 degrees, making the total snapshot count at almost 108000. Given the short period for this research, such a number would be nearly impossible and tremendously laborious to complete. Therefore we decided to make a movie from the snapshots. The movie was a time evolution of the snapshots. We just then changed the node angle to determine the best match. The selection criteria from the movie were simple; we compared the apparent structures such as the central bar, arms, and overall significant dispersion throughout with the CO emission snapshot. However, to make a more detailed comparison, we imposed a sky projection on the best-matched snapshot from the movie. Three iso-ellipticals, which represented the sky projection, were placed from the central region to the arms of the snapshots. Then, we made a detailed analysis of the structures on the interior and exterior of the sky projection. The results are discussed further in the discussion section(section 3)..

3.2   Simulation Snapshot, TW Method and Pattern Speed

This segment ties the simulation snapshots to the theoretical part of the research. We tried determining the pattern speed of the galaxy using the TW method. The TW method that we used for this segment was a refined version of the original TW method. The equation can be written as:

$$\Omega_p = \frac{1}{\sin i} \frac{<V(x)>}{<x>}$$

The numerator is the intensity weighted average line of sight of velocity, and the denominator is the intensity weighted average of the major axis multiplied by the sine of inclination angle. These parameters can be derived from the data cubes of the best snapshots. First, we converted the best-matched snapshots to fits files. We then made a separate python script to read the fits files. The header of the fits file included data about the pixels and intensity increments in x, y, and vz direction. After reading the pixel values from the header of the fits files, we generated velocity and x-axis cubes by reshaping the pixels from the fits files in three dimensions and multiplying each pixel with the intensity increments.

Then the 3D cubes were intensity weighted by dividing the intensity and axis cubes over the intensity cube. This procedure created a two-dimensional array with a lot of NaN values. The NaN value already existed in the original fit files, so they were just carried on after the computation. We replaced The NaN values with zeros and the integrated the two-dimensional array. This produced the parameters, $< V(x) >$ and $< x >$, required for determination of the pattern speed. A plot of $< V(x) >$ $vs.$ $< x >$ was then generated with a line of best fit. The slope of the line divided by the $\sin i$ provided the pattern speed of the galaxy as per the equation derived by Merrifield and Kuijken [1995]. The results we obtained and the constraints in the overall procedure are discussed in the discussion section.

4 Results

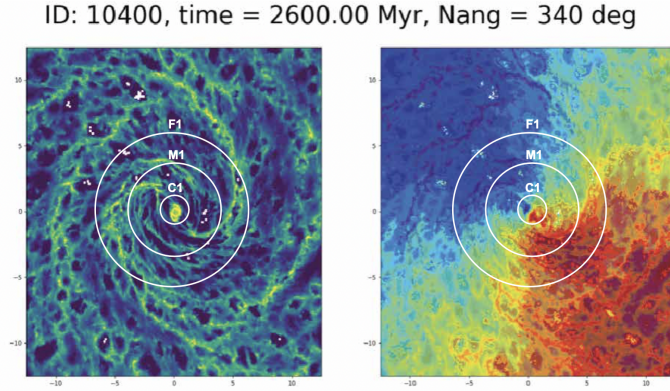## 4.1 Best Comparison Snapshots

Figure: ID 10400, Node Angle 340° : Central region C1 is almost vertical like the emission. In M1, the angular alignment of the bar region is also quite similar; dispersion, however, is not the same mainly due to the gas-particle simulation. At F1, The two arms are quite apparent however the right arm does not have proper pitch angle. It drops straight to the bar whereas it should have wound more closer to it. The left arm looks quite similar to the emission in both placement and density. This plot has proper dispersions but lacks appropriate windings of the structures. For the velocity plot, the central region in C1 has a prominent red region. However, there is no independent blue region. Dispersions accompany the blue region from other blue distributions from M1. The dispersion in M1, F1 and beyond is vast and has similarities to the emission.

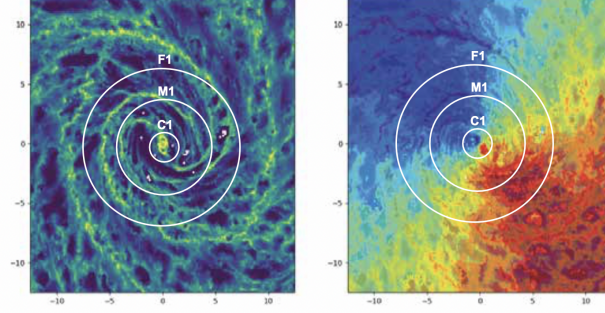ID: 10500, time = 2625.00 Myr, Nang = 280 deg

Figure: ID 10500, Node Angle 280°: In C1, the Central region is an exception-
ally prominent and vertical contributing similarity to the emission. In the M1
area, the angular alignment of the bar resembles a resemblance to the emission.
In the F1 region, the two arms are pretty apparent and winds closer to the bar.
However, similar to the previous plot, the arms lack some density dispersion
inside F1. In region C1 of the velocity plot, the red structure is quite prominent
and independent. However, the blue structure is not independent since the blue
dispersions in the M1 region accompany it. The overall stretch in the red region
in C1, M1, F1, and beyond is constrained. This segment deviates from the
main observation, where the dispersion of the prominent red areas is vast. The
overall stretch of the blue regions matches the emission. The overall velocity
fluctuations are also similar throughout the plot.

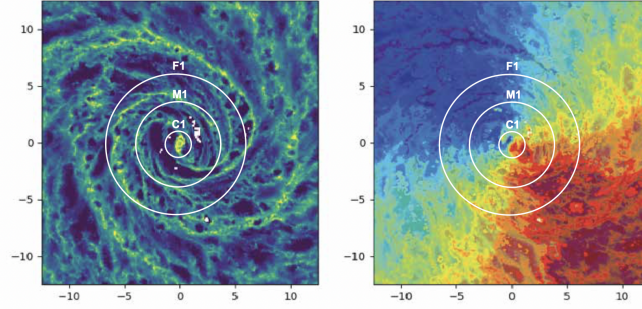ID: 10540, time = 2635.00 Myr, Nang = 260 deg

Figure: ID 10540,Node Angle 260°:The central and bar structure, region C1
and M1, are apparent. The most significant aspect of this density plot is the
winding of the right major arm, especially on the outskirts of the region F1.
The arm is woundcloser to the center and has a dip in density right before the
tail. This trend can be observed in the emission as well. However, the density
dispersion is not that great in both left and right arms, especially inside the F1
region, where we expect massive density fluctuations of the arms. The C1 region

has a prominent small blue region and a sizeable red region for the velocity plot. However, both the structures are not independent since dispersions from the M1 region accompany them. Hence the velocity dispersion in the galactic center deviates from observation. In the M1 region, there is a slight rightward stretch in the blue area, which shows some similarity to the CO emission; however, it is not quite prominent. The overall dispersion shows similarity throughout.
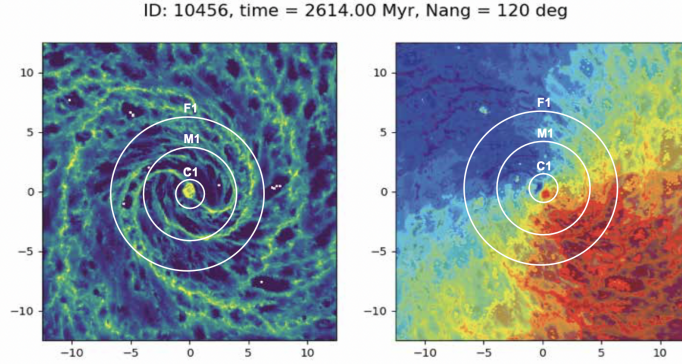

ID: 10456, time = 2614.00 Myr, Nang = 120 deg

Figure: ID 10456,Node Angle 120°: The most significant aspect of this plot is the winding of the bar structure near the F1 regions. They wound very close to the bar, which remarkably resembles the observation. In addition, the density dispersion in the right arm is better than in the previous plots. In region M1, there is a bar component, although it is not entirely apparent since it lacks some density dispersion. In C1, the core component has a significant amount of density dispersion which matches with the observation. In the C1 region of the velocity plot, there are two very distinct large red and small blue structures. These structures resemble a similarity with the emission. The overall dispersions also stretch out prominently in regions M1, F1, and beyond, making the general dispersions similar throughout the plot. Therefore, this is a good candidate for the velocity emission.
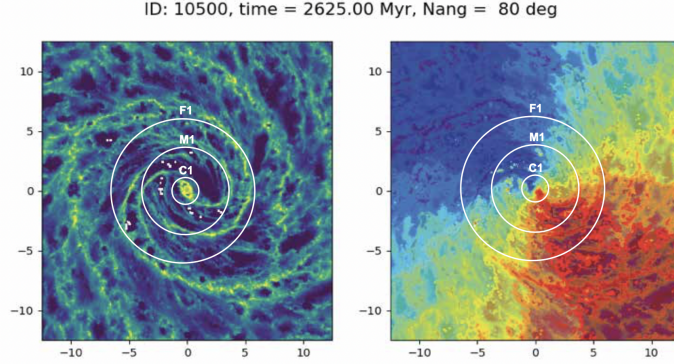

ID: 10500, time = 2625.00 Myr, Nang = 80 deg

Figure: ID 10500,Node Angle 80° :TThe left spiral arm that pass through region M1, closely resembles one present in the observed data, however it does curve inward significantly more (a search for snapshop where this was not the case yielded no results). Inside M1, the bar structure of the galactic center is clear and oriented correctly. The tail of the right spiral arm outside region F1, has a sharp edge that resembles a similar curvature in the observed data The velocity map decently resembles the observed velocity map, but not more so than other images. In particular, the crescent shape formed in M1, created by the boundary between higher (green) and lower (blue) velocity is a notable match. Local minima trails within the extreme low (blue) and high (red) velocity regions from all over the plot approximately correspond with trails in observation
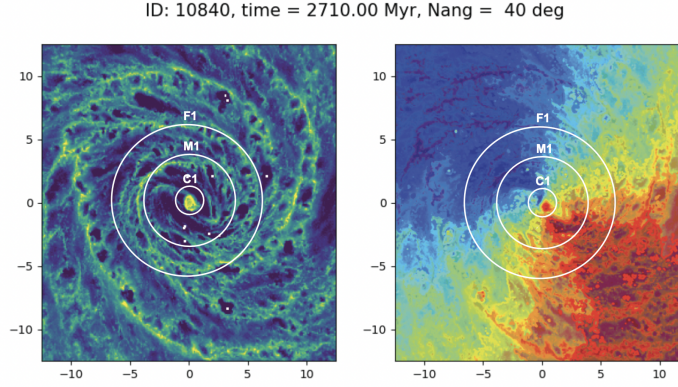

ID: 10840, time = 2710.00 Myr, Nang = 40 deg

Figure: ID 10840,Node Angle = 40° :This snapshot occurs late in the simulation, setting it apart from many of the others. The spiral arm structure is not strongly defined in the central region, which contrasts with the observed data.In region M1, while the galactic center does maintain a slight bar component, the spiral arms instead extend from a circular shape surrounding the center. In region F1, the spiral arms themselves are also twisted far more than in earlier snapshots, which does not perfectly align with observation. There are several distinct features that correspond with observation, however. The right spiral arm which extends beyond F1 flattens and then rigidly changes direction downward, creating a "kink" in the arm. Additionally, the left spiral arm inside F1, with the bottom arm fading in mass shortly after the split while the top arm continues as a dominant structure toward the top of the galaxy. The structures of the right arm inside F1 region, also indicates a section where the spiral arms blend with each other and the surroundings. The velocity map has a number of important matching features, as well. The 3 local minima trails in the high velocity (red) section, of C1, M1 and F1, match adequately with the corresponding trails in the observed data. The galactic center also accuratelymatches observation, with a low velocity point on the left and high velocity point on the right, as well as a trail of low velocity slightly farther to the right.
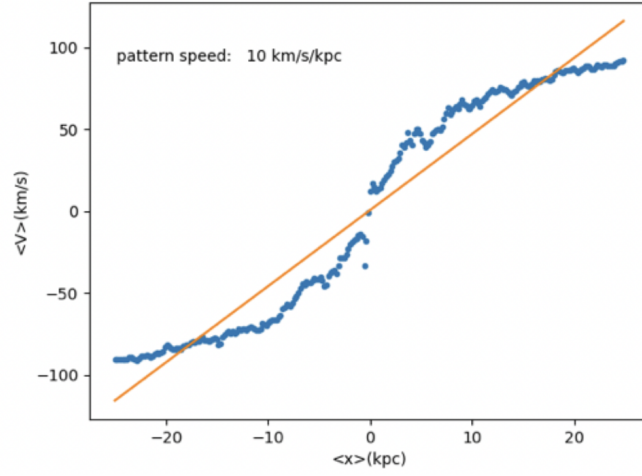
4.2 Pattern Speed from TW method

Figure: Gas Particle Simulation ID 10456, Node Angle 120° and Position Angle 90° up to 25 kpc(arm region included)
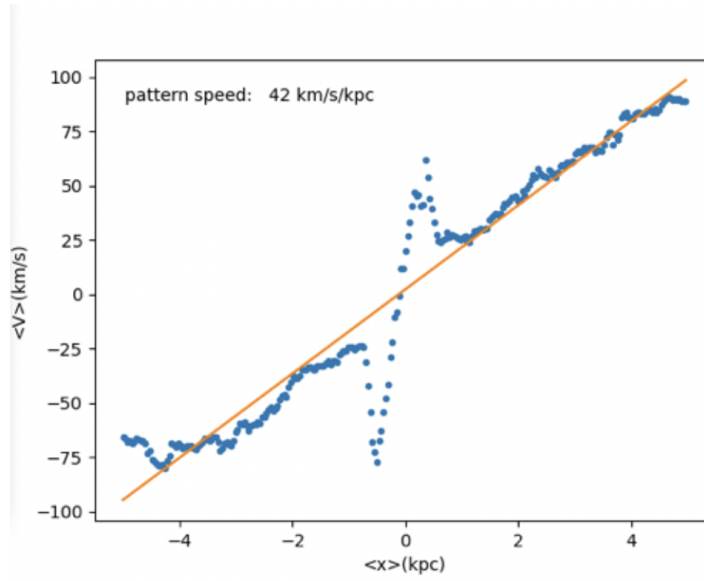

Figure: Gas Particle Simulation ID 10456, Node Angle 120° and Position Angle 90° up to the bar region

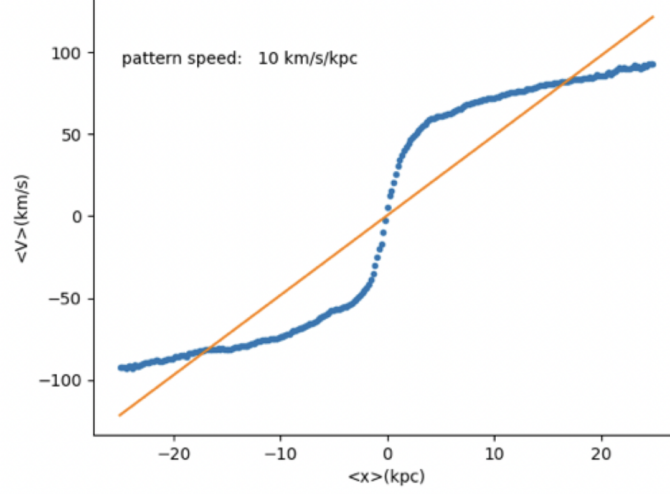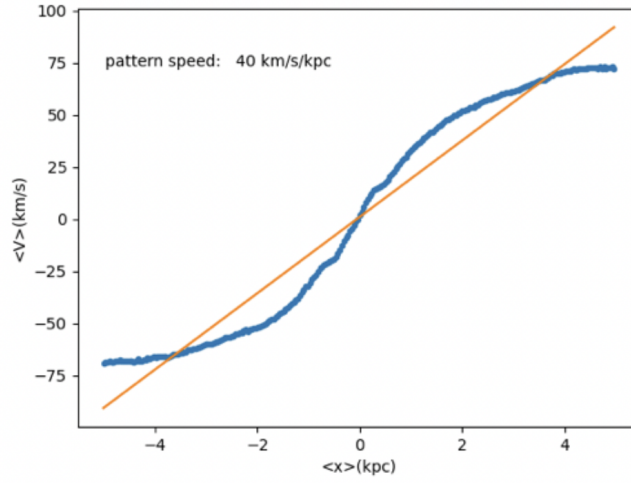Figure: Star Particle Simulation ID 10456, Node Angle 120° and Position Angle 90° upto 25 kpc(arm region included)

Figure: Star Particle Simulation ID 10456, Node Angle 120° and Position Angle 90° upto the bar region

5 Discussion

We did not determine a single simulation snapshot that completely resembles the CO emission of M83. However, we found multiple snapshots which displayed

some brilliant intrinsic features that matched the emission. For example, Plot ID10500 at Node Angle 280° and Plot ID10540 had a good match for the right arm. However, Plot ID 10456 at Node Angle 120° had a good match for the left arm. We also had few plots that showed excellent density dispersion, e.g., Plot ID 10400 at node angle 340°. Some of the plots had excellent velocity dispersion, such as ID 500 at Node angle 80°. Therefore one single plot could not be isolated as a candidate for the exact match, but multiple snapshots were used as candidates for the best matches.

The TW method was applied to both gas and star particle simulation of Simulation ID 10456. It was one of the best matches. Gas Particle Simulation of ID 10456 at Node Angle 120° and Position Angle 90° upto bar region (around 4 kpc) gave a pattern speed of 42 km/s/kpc and the same simulation but with star particles gave pattern speed of 40 km/s/kpc. The simulation pattern speeds were significantly closer to the value determined as 45±8 km/s/kpc by [Zimmer et al., 2004], who used observation data. Our results from the bar and the arm region show a declining trend in pattern speed as the distance from the center is increased. When the TW method was applied to the arm region it dropped down to 10 km/s/kpc for both star and gas particle simulations. This trend somewhat deviates from the assumption of a global pattern speed as suggested by the Density Wave Theory. However future analysis may provide more fruitful conclusions to this trend. The plot from star particle simulation was more smoother than the gas particle simulation which should also be a good point for analysis in future prospects.

This research has abundant potential in case it is to be continued in the future. Error analysis could be applied to the TW method for a more conclusive result. The overall TW method also can be adjusted further to make better approximations of the pattern speed. More simulation plots can be used for the TW method to increase the reliability of the pattern speed. The TW method can also be applied to the CO emission directly for a better comparison with the simulation data.

References

C. C. Lin and F. H. Shu. On the Spiral Structure of Disk Galaxies. *Astrophysical Journal*, 140:646, Aug. 1964. doi: 10.1086/147955.

M. R. Merrifield and K. Kuijken. The pattern speed of the bar in NGC 936. *Monthly Notices of the Royal Astronomical Society*, 274(3):933–938, June 1995. doi: 10.1093/mnras/274.3.933.

S. Tremaine and M. D. Weinberg. Dynamical friction in spherical systems. *Monthly Notices of the Royal Astronomical Society*, 209:729–757, Aug. 1984. doi: 10.1093/mnras/209.4.729.

P. Zimmer, R. J. Rand, and J. T. McGraw. The Pattern Speeds of M51, M83,

and NGC 6946 Using CO and the Tremaine-Weinberg Method. *Astrophysical Journal*, 607(1):285–293, May 2004. doi: 10.1086/383459.